Rate-Adaptive Modulation and Low-Density Parity-Check Coding for Optical Fiber Transmission Systems

Gwang-Hyun Gho and Joseph M. Kahn

***Abstract*—We propose a rate-adaptive optical transmission scheme using variable-size constellations at a fixed symbol rate and variable-rate forward error correction (FEC) codes with soft-decision decoding (SDD), quantifying how achievable bit rates vary with transmission distance. The scheme uses outer Reed–Solomon codes and inner extended irregular repeat-accumulate low-density parity-check (LDPC) codes to vary the code rate, combined with single-carrier polarization-multiplexed M-ary quadrature amplitude modulation with variable M and digital coherent detection. LDPC codes are decoded iteratively using belief propagation. Employing M = 4,8,16, the scheme achieves a maximum bit rate of 200 Gbit/s in a nominal 50-GHz channel bandwidth. A rate adaptation algorithm uses the signal-to-noise ratio (SNR) or the FEC decoder input bit-error ratio (BER) estimated by a receiver to determine the FEC code rate and constellation size that maximize the information bit rate while yielding a target FEC decoder output BER and a specified SNR margin. We simulate single-channel transmission through long-haul fiber systems with or without inline chromatic dispersion compensation, incorporating numerous optical switches, evaluating the impact of fiber nonlinearity and bandwidth narrowing. With zero SNR margin, we achieve bit rates of 200/100/50/20 Gbit/s over distances of 960/2800/4400/9680 km and 1920/4960/8160/19,360 km in dispersion-compensated and -uncompensated systems, respectively, corresponding to an increase of about 50% in reach compared to a reference system that uses a hard-decision FEC scheme. Compared to an ideal coding scheme, the proposed scheme exhibits a performance gap ranging from about 4.0 dB at 960 km to 2.7 dB at 9680 km in compensated systems, and from about 3.9 dB at 1920 km to 2.9 dB at 19,360 km in uncompensated systems. Observed performance gaps are about 2.5 dB smaller than for the reference hard-decision FEC scheme, close to the improvement expected when using SDD.**

***Index Terms*—Adaptive modulation; Coherent detection; Forward error correction; Information rates; Optical fiber communication; Quadrature amplitude modulation; Variable-rate codes.**

I. Introduction

Modern wireline and wireless communication systems use rate-adaptive transmission, trading off spectral efficiency for reliability. Depending on the channel conditions, which are often time varying, the link parameters are adjusted, including the constellation size, forward error correction (FEC) code rate, used bandwidth and power allocation. In contrast, to date, commercial optical transmission systems have employed fixed bit rates.

Rate-adaptive optical transmission techniques can enable increased bit rates over shorter links, while enabling transmission over longer links when regeneration is not available. They are likely to become more important with increasing network traffic and a continuing evolution toward optically switched mesh networks with flexible transceivers and switches [1], which make signal quality more variable. Rate-adaptive optical transmission could help improve network robustness, flexibility and throughput.

Variable-rate transmission using variable-rate codes with fixed constellations was proposed in [2], and was extended to variable-size constellations in [3]. References [2,3] report the use of hard-decision FEC decoding. FEC schemes in optical communications have evolved over several generations [4], starting from a single block code with hard-decision decoding (HDD), followed by concatenated block codes and more recently iterative soft-decision decoding (SDD) of various constituent codes [5,6], seeking the highest possible coding gain. In this paper, we propose variable-size constellations and variable-rate FEC codes with SDD, achieving higher coding gain than in [3]. Variable-rate transmission using SDD FEC was recently studied in [7], employing quasi-cyclic low-density parity-check (LDPC) codes with rates from 0.67 to 0.92, combined with variable-size quadrature amplitude modulation (QAM) constellations. In our FEC scheme, instead of using LDPC codes only, we concatenate them with outer HDD codes in order to mitigate potential error floors of SDD FEC codes, similar to [8,9]. We also provide a wider range of code-rate variation and use a different method for constructing LDPC codes than in [7]. In systems with or without inline chromatic dispersion (CD) compensation, we quantify the achievable information bit rate versus distance and estimate the performance gap between the proposed scheme and an ideal coding scheme that achieves information-theoretic limits. We also compare the results of this paper to those in [3] in order to quantify performance improvements between hard- and soft-decision FEC schemes.

This paper is organized as follows. In Section II, we describe the proposed scheme using variable-rate codes and variable-size constellations, and a rate adaptation algorithm that uses the measured signal-to-noise ratio (SNR) or bit-error

Manuscript received May 17, 2012; revised July 29, 2012; accepted August 14, 2012; published September 20, 2012 (Doc. ID 168124).

The authors are with the E. L. Ginzton Laboratory, Department of Electrical Engineering, Stanford University, Stanford, California 94305-4088, USA (e-mail: ggho@alumni.stanford.edu).

Digital Object Identifier 10.1364/JOCN.4.000760

ratio (BER) to determine the maximum information bit rate that can be supported. In Section III, we describe simulations of the rate-adaptive scheme in a model terrestrial network. In Section IV, we present simulation results, including achievable information bit rates as a function of distance, with or without CD compensation. In Section V, we discuss observed trends of SNR versus distance and compare the performance of the proposed scheme to information-theoretic limits. We present conclusions in Section VI.

II. Rate-Adaptive Modulation and Coding Scheme

A. Variable-Size Constellations

We use polarization-multiplexed M-ary QAM (PM-M-QAM) with modulation orders $M = 4, 8, 16$. We use Gray mapping for 4- and 16-QAM square constellations and an optimal bit mapping [10] for the 8-QAM cross constellation, as shown in Fig. 1.

B. Variable-Rate FEC Coding Scheme

Our FEC scheme uses concatenated Reed–Solomon (RS) codes and LDPC codes, referred to as RS–LDPC codes throughout the remainder of this paper. An LDPC code is a linear block code defined by a parity-check matrix containing a low density of one bits, and which can achieve performance approaching information-theoretic limits [11]. At very low error rates, LDPC codes exhibit error floors that become more difficult to avoid at high code rates and moderate block lengths [12], so we add a high-rate outer RS code to reduce error floor effects, as in [9]. An RS code is a linear block code with strong capability to correct both random and burst errors [13]. In an RS–LDPC code, the inner LDPC code provides most of the coding gain.

We employ a family of variable-rate LDPC codes that are used in second-generation digital video broadcasting (DVB-S2), which broadcasts high-speed data from satellites to mobile devices [8]. The DVB-S2 LDPC codes are designed using an extended irregular repeat-accumulate (eIRA) method that is suitable for producing high-rate codes offering good performance and reduced encoding complexity (which can be high for general LDPC codes) [14]. The DVB-S2 standard provides ten codes with codeword lengths of 16,200 bits and code rate ranges from about 0.25 to 0.9. We choose six codes, where the highest rate code, with code rate 0.89, offers a net coding gain of about 10.5 dB at a decoded BER of 10^{-13}, comparable to third-generation FEC codes for optical communications [4]. Here, we perform iterative SDD using the belief propagation (BP) algorithm [15]. The rates of our constructed codes and their performance for $M = 4, 8, 16$ on an additive white Gaussian noise (AWGN) channel are shown in Fig. 2, where n_{LDPC} and k_{LDPC} indicate the lengths in bits of the codeword and message word, respectively.

There are several options for generating variable-rate LDPC codes. First, one can use different codes for different code rates. This approach increases encoder/decoder hardware complexity. Second, one can puncture a low-rate mother code to generate higher-rate codes [16]. Puncturing is effective typically over only a small range of code rates, and puncturing patterns must be carefully chosen to prevent performance degradation. Third, one can shorten a high-rate mother code to generate lower-rate codes [17]. Shortening results in a code with a shorter message word length as compared to codes having the same code rate but having codeword length equal to that of the mother code, which prevents construction of very high-rate outer RS codes that have a fixed error correction capability. Shortening also reduces the codeword length (as compared to the mother code), which mandates higher decoder throughput requirements at lower information bit rates. Fourth, one can employ various puncturing-and-extending methods, as proposed in [18,19], but these exhibit some limitations, such as limited supported code rate ranges and increased decoder complexity. Based on these considerations, we have chosen to use different LDPC codes for different rates, utilizing verified good codes at each different rate, avoiding a long search time

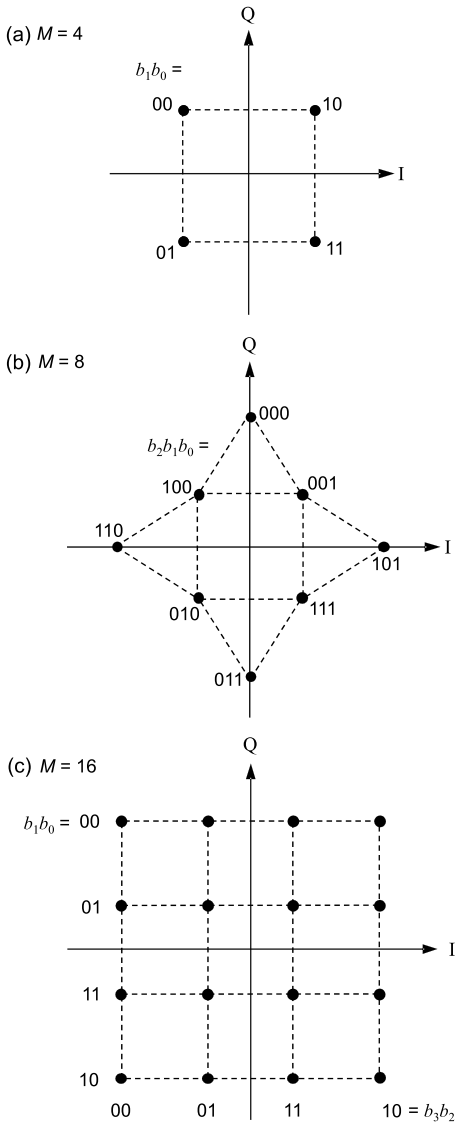

Fig. 1. QAM constellations with bit-to-symbol mappings. (a) Square 4-QAM. (b) Cross 8-QAM. (c) Square 16-QAM.

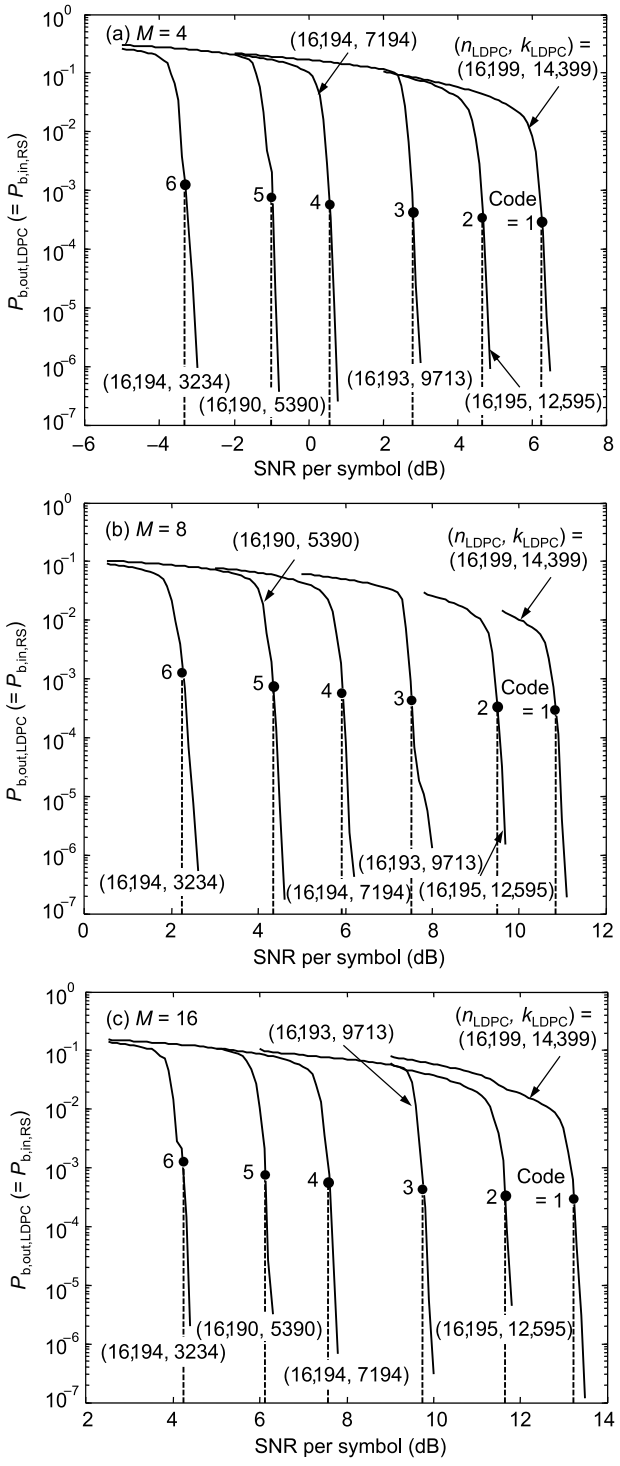

Fig. 2. Performance of inner LDPC codes on an AWGN channel with six different rates, in terms of LDPC decoder output BER versus SNR per symbol. The BP algorithm uses 50 iterations. The SNR per symbol is measured at the equalizer output (i.e., the LDPC decoder input) and $P_{b,\text{out,LDPC}}$ is measured at the LDPC decoder output (i.e., the RS-encoder input). (a) $M = 4$. (b) $M = 8$. (c) $M = 16$.

to find good puncturing patterns, minimizing the overheads when concatenating with outer RS codes, and minimizing the decoder throughput requirements.

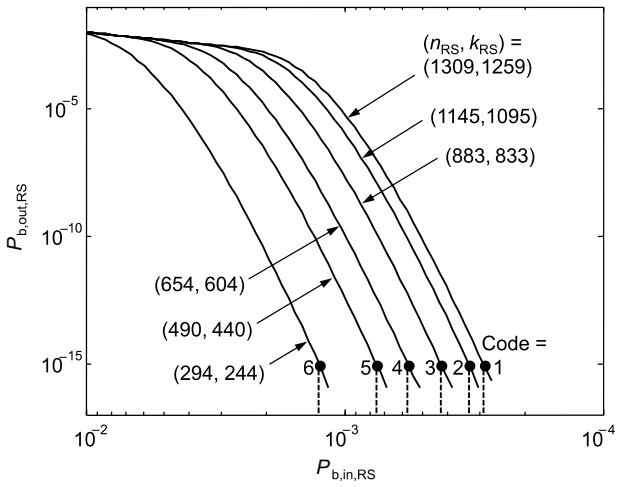

Fig. 3. Performance of outer RS codes with six different rates, in terms of input and output BERs of the RS decoder. The $P_{b,\text{in,RS}}$ and $P_{b,\text{out,RS}}$ values are measured at the input and output of the RS decoder, respectively.

We employ, as outer codes, RS codes offering an error correction capability of 25 symbols. A family of variable-rate RS codes in GF(2^{11}) is constructed by shortening a mother code that has a highest rate of 0.98. Note that the RS shortening does not induce any additional decoder throughput requirements, which is determined by the length of the inner LDPC codeword. We employ HDD of the RS code [13]. The rates and performance of our constructed codes are shown in Fig. 3, where n_{RS} and k_{RS} indicate the length of the codeword and message word in units of 11 bits, respectively, and $P_{b,\text{in,RS}}$ and $P_{b,\text{out,RS}}$ are input and output BERs of the RS decoder. The curves in Fig. 3 have been calculated analytically assuming independent errors and no decoding failures [20].

We linearly interleave RS-encoded bits prior to LDPC encoding. To align the number of RS-encoder output bits (n_{RS}) to the number of LDPC-encoder input bits (k_{LDPC}), we perform a shortening of DVB-S2 LDPC codes (by less than 11 bits). The code parameters for RS and LDPC codes are listed in Table I, where k_m denotes the length of the message word for the mother code (the codeword length for the mother code, n_m, can be calculated as $n_m = k_m + n - k$). The encoding procedure of RS–LDPC codes is illustrated in Fig. 4.

We assume that line encoding and RS–LDPC encoding are performed on a single serial bit stream, after which bits are mapped in round-robin fashion to the 2 $\log_2 M$ tributaries of the PM-M-QAM signal as in [3].

C. Rate Adaptation Algorithm

Given a symbol rate R_s, an RS–LDPC code rate r_C, a line code rate r_L, and a modulation order M, the information bit rate R_b can be calculated as

$$R_b = 2 r_L r_C R_s \log_2 M, \tag{1}$$

assuming PM transmission.

TABLE I
RS AND LDPC CODE PARAMETERS: LENGTHS OF MESSAGE WORD AND CODEWORD

Code	$k_{\mathrm{RS}}(k_{\mathrm{RS}},m)$	n_{RS}	$k_{\mathrm{LDPC}}(k_{\mathrm{LDPC}},m)$	n_{LDPC}	r_C
1	1259 (1997)	1309	14,399 (14,400)	16,199	0.855
2	1095 (1997)	1145	12,595 (12,600)	16,195	0.744
3	833 (1997)	883	9713 (9720)	16,193	0.566
4	604 (1997)	654	7194 (7200)	16,194	0.410
5	440 (1997)	490	5390 (5400)	16,190	0.299
6	244 (1997)	294	3234 (3240)	16,194	0.166

Notes.
The notation is defined in the text.

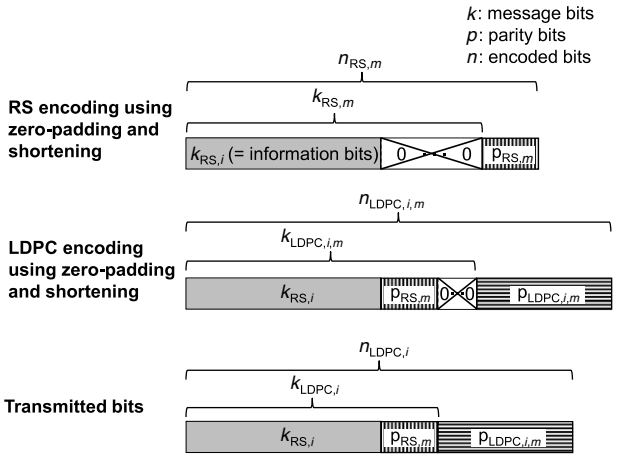

Fig. 4. Constructing variable-rate inner RS and outer LDPC codes by shortening the mother codes. The overall RS–LDPC encoding process is also illustrated.

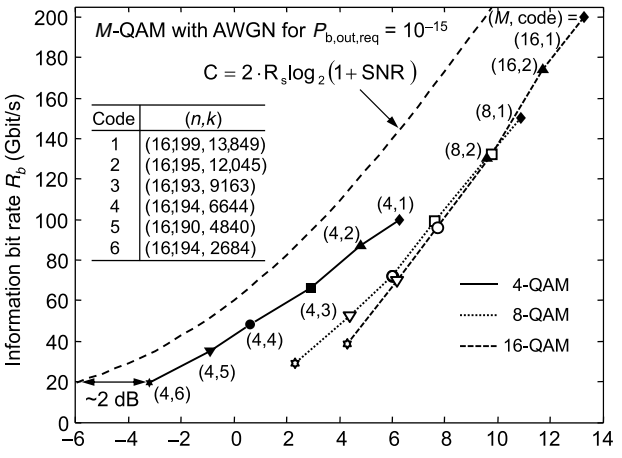

Fig. 5. Information bit rate versus threshold SNR per symbol for PM-M-QAM on an AWGN channel. Information bit rates are computed using Eq. (1), while SNR values are obtained by combining Figs. 2 and 3. The set of filled (M, code) combinations represent a possible choice of modes for rate-adaptive transmission.

We quantize the achievable bit rate R_b into multiple segments $R_{b,i}, i = 1,2,\ldots,N_s$, where $R_{b,i} > R_{b,i+1}$. Each $R_{b,i}$ can be represented by a set of transmission parameters $(M,r_C)_i$, commonly referred to as a mode. For each transmission mode, we define a threshold value for channel state information (CSI), $\mathrm{CSI}_{th,i}$, at which $(M,r_C)_i$ can achieve a target decoder output BER, $P_{b,\mathrm{out,req}}$, on an AWGN channel. The transmitter monitors variations of CSI estimated and reported by the receiver, and adjusts the RS–LDPC code rate and constellation size to maximize R_b, while achieving the target BER $P_{b,\mathrm{out,req}}$ at the RS decoder output. We consider two possible choices for CSI: (a) SNR, which is the SNR per symbol estimated at the equalizer output, or (b) $P_{b,\mathrm{in,RS}}$, which is the BER measured at the RS decoder input (LDPC decoder output). We design the rate adaptation algorithm such that it can provide an arbitrary specified SNR margin μ (in dB).

Figure 5 shows information bit rates and threshold values of SNR for different combinations of (M,r_C) on an AWGN channel. Information bit rates are computed using Eq. (1), and required SNR values are obtained by combining Figs. 2 and 3 with $P_{b,\mathrm{out,req}} = 10^{-15}$. The filled (M,r_C) combinations represent a possible choice of transmission modes using SNR as CSI. The transmission modes using $P_{b,\mathrm{in,RS}}$ as CSI can be defined as described in [2]. Figure 5 also shows the capacity of an ideal discrete-time AWGN channel transmitting at symbol rate R_s in two polarizations, which is computed by the formula

$$C = 2R_s \log_2(1+\mathrm{SNR}). \quad (2)$$

In Fig. 5, we observe that, at high SNR, the gap to capacity increases because unshaped uniformly spaced QAM is not a capacity-achieving modulation scheme [21,22], and that, at low SNR, the gap to capacity increases for higher M because the bit mappings employed here result in unequal bit-error protection for higher-order modulation [23].

A pseudocode for the rate adaptation algorithm (similar to II.C of [3]) is given as follows, where $\mathrm{CSI}_{th,i}\{\Delta_i,\mu\}$ denotes a threshold CSI value for mode i considering SNR penalty Δ_i and SNR margin μ:

1) Initialize parameters to the highest rate mode.
   - Initialize mode: $(M,r_C)_i \rightarrow (M,r_C)_1$
   - Initialize up/down counters: $C_{\mathrm{up}} = C_{\mathrm{down}} = 0$
2) Check if rate change is necessary.
   - if reported CSI satisfies $\mathrm{CSI}_{th,i-1}\{\Delta_i,\mu_{\mathrm{up}}\}$
     - $C_{\mathrm{up}} = C_{\mathrm{up}} + 1$
     - if $C_{\mathrm{up}} \geq N_{\mathrm{up}}$, $(M,r_C)_i \rightarrow (M,r_C)_{i-1}$
   - else if reported CSI does not satisfy $\mathrm{CSI}_{th,i}\{\Delta_i,\mu_{\mathrm{down}}\}$
     - $C_{\mathrm{down}} = C_{\mathrm{down}} + 1$
     - if $C_{\mathrm{down}} \geq N_{\mathrm{down}}$, $(M,r_C)_i \rightarrow (M,r_C)_{i+1}$
   - else
     - $C_{\mathrm{up}} = C_{\mathrm{down}} = 0$
     - $(M,r_C)_i \rightarrow (M,r_C)_i$
3) Go to step 2.

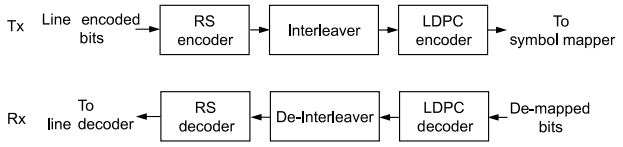

Fig. 6. FEC chain for encoding and decoding concatenated RS–LDPC codes.

In this pseudocode, the reported CSI "satisfies" CSI_{th} if $\mathrm{CSI} > \mathrm{CSI}_{th}$ when using the SNR as CSI, and if $\mathrm{CSI} < \mathrm{CSI}_{th}$ when using $P_{b,\mathrm{in,RS}}$ as CSI. The parameters μ_{up} and μ_{down} are SNR margins when changing the rate up and down, respectively, and N_{up} and N_{down} are counters when changing the rate up and down, respectively. When using $P_{b,\mathrm{in,RS}}$ as CSI, threshold values of $P_{b,\mathrm{in,RS}}$ may be estimated from the curves for AWGN channels in Fig. 2, and SNR penalty parameters are not required [2].

III. System Simulations

We have evaluated the rate-adaptive transmission scheme in the same model long-haul system as shown in Fig. 6 of [3], but using a different FEC scheme, which is described in Fig. 6.

We simulated a single channel in a wavelength-division-multiplexed system with a center wavelength of 1550 nm and nominal 50-GHz channel spacing. The modulation is single-carrier PM-M-QAM using non-return-to-zero pulses at a symbol rate of R_s = 30.156 Gsymbols/s. Each modulator is a quadrature Mach–Zehnder device. Each drive waveform is a train of rectangular pulses filtered by a five-pole Bessel low-pass filter having a 3-dB bandwidth of $1.4R_s$ = 42.2 GHz. Percentages of 90%, 95% and 99% of the modulated signal energy are contained in bandwidths of 29.3, 33.7 and 41 GHz, respectively. We employ line coding at rate of r_L = 64/66, yielding an information bit rate of R_b = 200 Gbit/s for the highest overall code rate of r_C and $M = 16$.

The fiber network comprises multiple 80-km spans of standard single-mode fiber. In dispersion-compensated systems, dispersion-compensating fiber is used to pre-compensate the CD down to 3.1% residual dispersion per span (RDPS) using the same fiber parameters as provided in Table I of [3]. We use the same parameters for two-stage inline amplifiers, reconfigurable optical add–drop multiplexers (ROADMs) (inserted at every third span), and the multiplexer and de-multiplexer as provided in [2]. While typical networks would not have such a high density of ROADMs, especially over ultra-long-haul routes, we choose a homogeneous high-density distribution of ROADMs to be conservative and to obtain simple trends of achievable bit rate versus transmission distance.

The receiver employs a fifth-order Butterworth anti-aliasing filter of 3-dB bandwidth R_s, samples at a rate of $2R_s$ complex samples per polarization and performs digital compensation of CD and polarization-mode dispersion using finite impulse response time-domain filtering, as described in [24].

Signal propagation is simulated by numerical integration of the vector nonlinear Schrödinger equation by the split-step Fourier method [25].

We run the BP algorithm for LDPC decoding with 50 iterations. Then we measure $P_{b,\mathrm{in,RS}}$ at the RS decoder input (i.e., the LDPC decoder output). We simulate a sufficient number of symbols such that the true value of $P_{b,\mathrm{in,RS}}$ does not exceed 130% of the estimate with 95% confidence down to measured BERs of $P_{b,\mathrm{in,RS},95,M} = 1.9\times10^{-4}, 1.3\times10^{-4}$, and 9.5×10^{-5} for $M = 4, 8, 16$. We estimate that the uncertainty in measured $P_{b,\mathrm{in,RS}}$ corresponds to 0.1-dB uncertainty in SNR.

At each transmission distance, the launched power is optimized with 1-dB resolution to minimize the value of $P_{b,\mathrm{in,RS}}$. When the measured $P_{b,\mathrm{in,RS}}$ is below $P_{b,\mathrm{in,RS},95,M}$, the launched power is optimized to minimize the value of $P_{b,\mathrm{in,LDPC}}$ (or BER at the equalizer output) that is computed as described in [3]. We have found that in cases when the measured $P_{b,\mathrm{in,RS}}$ is above the threshold value, minimizing $P_{b,\mathrm{in,RS}}$ and minimizing $P_{b,\mathrm{in,LDPC}}$ result in the same optimized power in about 85% of the cases, and only a 1-dB difference in the remaining cases.

IV. Simulation Results

In order to evaluate the rate-adaptive scheme, at each transmission distance, for each modulation order, and for each RS–LDPC code, after the transmit power is optimized, the received SNR per symbol and RS decoder input BER are recorded. The SNR per symbol is estimated by calculating the ratio between the average symbol power and the noise variance, which is empirically measured at the equalizer output.

We have employed the rate adaptation algorithm of Subsection II.C, using $P_{b,\mathrm{in,RS}}$ as CSI, and using all possible transmission modes. We assume a required RS–LDPC decoder output BER $P_{b,\mathrm{out,req}} = 10^{-15}$, SNR margins $\mu_{\mathrm{up}} = \mu_{\mathrm{down}} = 0, 1, \ldots, 5$ dB and counter parameters $N_{\mathrm{up}} = N_{\mathrm{down}} = 1$ (because we assume static channel conditions). Figures 7(a) and 7(b) present achievable information bit rates with and without inline dispersion compensation, respectively, as a function of transmission distance. In dispersion-compensated systems, with zero margin, a bit rate R_b = 200 Gbit/s can be realized up to 960 km, with the achievable rate decreasing by approximately a factor of two for every additional 2000 km. In dispersion-uncompensated systems, with zero margin, a bit rate R_b = 200 Gbit/s can be realized up to 1920 km, with the achievable rate decreasing by approximately a factor of two for every additional 3000 km. Compared to the hard-decision FEC scheme of [3], the transmission distances have increased by about 50%. Our results can be compared to those in [26], where bit rates of 200 Gbit/s, 300 Gbit/s, and 400 Gbit/s are achieved at distances 6400 km, 3900 km, and 2100 km, respectively, but in a more optimistic scenario, using no protection against error floors, and using digital backward propagation to compensate for intrachannel nonlinearities.

We used $P_{b,\mathrm{in,RS}}$ as CSI, and found that the uncertainty of measured $P_{b,\mathrm{in,RS}}$ may result in a reduced transmission distance by at most two spans for dispersion-compensated systems for distances beyond 5000 km, but the penalty may increase to three spans for an uncompensated system for distances beyond 10,000 km.

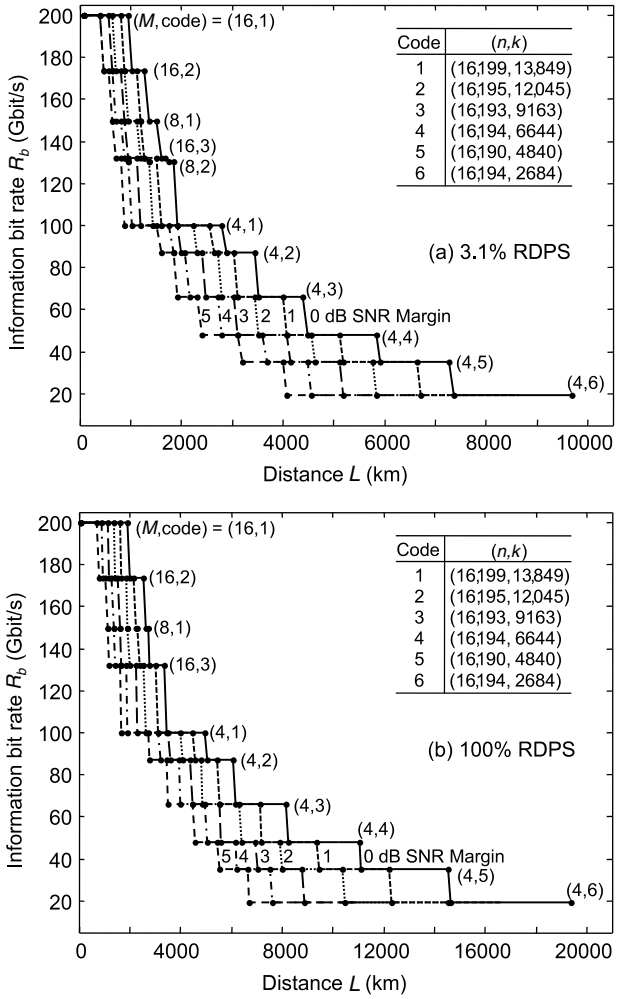

Fig. 7. Achievable information bit rates versus transmission distance for different SNR margins. The set (M, code) denotes the modulation order and type of RS–LDPC code. (a) Dispersion-compensated system. (b) Dispersion-uncompensated system.

V. Discussion

In this section, we examine how the SNR in the model system scales with transmission distance, and estimate the performance gap between the proposed rate-adaptive scheme and an ideal coding scheme achieving information-theoretic limits. We also discuss carrier phase synchronization, including laser linewidth requirements and how to avoid cycle slips.

We consider several different measures of the SNR and compare these to an equivalent SNR corresponding to the information bit rate achieved by the proposed rate-adaptive scheme. This discussion makes reference to Figs. 8(a) and 8(b), which describe dispersion-compensated and uncompensated systems, respectively. Each curve in Figs. 8(a) and 8(b) is computed for the information bit rates, transmission modes (FEC codes and modulation schemes) and transmission distances defined for 0-dB margin in Figs. 7(a) and 7(b)

The uppermost solid curves in Figs. 8(a) and 8(b) show $\mathrm{SNR}_{\mathrm{AWGN}}$, which is an empirical estimate of the SNR per symbol (in two polarizations) as limited only by the accumulated optical amplifier noise:

$$\mathrm{SNR}_{\mathrm{AWGN}} = \frac{P_t}{P_n}. \tag{3}$$

Here, P_t is the transmitted signal power, optimized at each transmission distance, which equals the received signal power at the de-multiplexer input, since the network is designed to have unit signal gain. P_n is the noise power in two polarizations, and is computed using (8) in [2]. The dashed curves in Figs. 8(a) and 8(b) show $\mathrm{SNR}_{\mathrm{AWGN,\ best\text{-}fit}}$ for dispersion-compensated and -uncompensated systems, respectively, which is a power-law fit to the observed $\mathrm{SNR}_{\mathrm{AWGN}}$ as a function of transmission distance L:

$$\mathrm{SNR}_{\mathrm{AWGN,\ best\text{-}fit}} = \begin{cases} \dfrac{A_c}{L^{1.40}}, & 3.1\%\ \mathrm{RDPS} \\ \dfrac{A_u}{L^{1.15}}, & 100\%\ \mathrm{RDPS}. \end{cases} \tag{4}$$

The constants A_c, A_u and the exponent of L have been found by curve fitting. We obtained trends of $\mathrm{SNR}_{\mathrm{AWGN}}$ similar to those in [3]. In the dispersion-compensated system, $\mathrm{SNR}_{\mathrm{AWGN}}$ scales as $L^{-1.40}$, a slightly weaker dependence than in systems using a fixed polarization-multiplexed quadrature phase-shift keying constellation [2], where the dependence was found to be $L^{-1.55}$. In the dispersion-uncompensated system, the $L^{-1.15}$ dependence is consistent with [27], where the optimized SNR was found to scale as L^{-1}.

The middle solid curves in Figs. 8(a) and 8(b) show $\mathrm{SNR}_{\mathrm{AWGN+NL,equivalent}}$ for dispersion-compensated and uncompensated systems, respectively, which is the SNR per symbol observed empirically at the equalizer output, and includes all linear noise (amplifier noise and equalizer noise enhancement) and "noise" arising from fiber nonlinearity. At small L, $\mathrm{SNR}_{\mathrm{AWGN+NL,equivalent}}$ is about 3.1 dB and 4.2 dB lower than $\mathrm{SNR}_{\mathrm{AWGN}}$ for dispersion-compensated and -uncompensated systems, respectively, indicating that, at the optimum P_t, the amplifier noise and nonlinear noise powers are roughly equal. At large L, the difference increases to about 5.9 dB and 8.6 dB for dispersion-compensated and -uncompensated systems, respectively. Presumably, the increase is caused by propagation through many cascaded ROADMs over long distances, which causes bandpass filtering of the signal. When this filtering is compensated by the linear equalizer, noise enhancement occurs. The noise enhancement at large L is more pronounced here as compared to that in [3], because the SDD FEC scheme here allows the signal to propagate over longer distances than the HDD FEC scheme used in [3].

The bottom solid curves in Figs. 8(a) and 8(b), $\mathrm{SNR}_{\mathrm{required,ideal}}$, are computed by inverting Eq. (2):

$$\mathrm{SNR}_{\mathrm{required,ideal}} = 2^{\frac{R_b}{2R_s}} - 1. \tag{5}$$

$\mathrm{SNR}_{\mathrm{required,ideal}}$ corresponds to the SNR required for an ideal capacity-achieving coding scheme to achieve error-free transmission on an AWGN channel at the information bit rate R_b achieved by the proposed scheme with zero SNR margin in Fig. 7. The vertical separation between

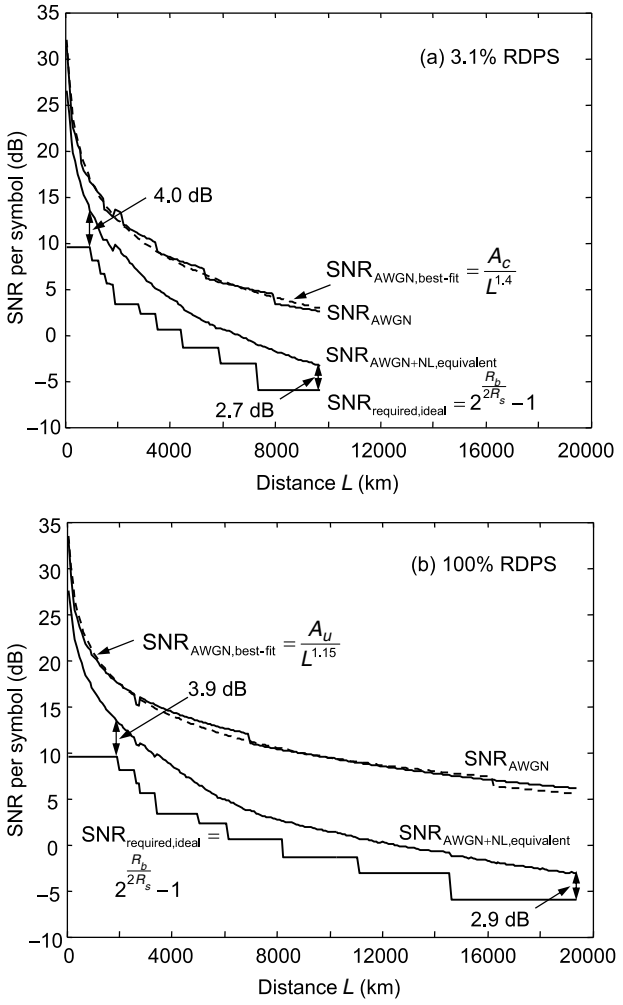

Fig. 8. Two different measures of SNR compared to the SNR required for an ideal capacity-achieving coding scheme to achieve error-free transmission at the information bit rate R_b achieved by the proposed rate-adaptive scheme. (a) Dispersion-compensated system. (b) Dispersion-uncompensated system.

$\mathrm{SNR}_{\mathrm{AWGN+NL,equivalent}}$ and $\mathrm{SNR}_{\mathrm{required,ideal}}$ is an estimate of the performance gap between an ideal coding scheme and the scheme proposed here. For dispersion-compensated systems, the gap ranges from about 4.0 dB to about 2.7 dB as L varies from 960 to 9680 km, as shown in Fig. 8. For dispersion-uncompensated systems, the gap ranges from about 3.9 dB to about 2.9 dB as L varies from 1920 to 19,360 km.

A summary of the performance gaps for different FEC schemes, channel types, and residual dispersion values is provided in Table II. Several observations about these performance gaps can be made.

First, the gaps at small L, where higher modulation orders are used, are larger by about 1 dB than the gaps at large L, where lower modulation orders are used. We expect that, at small L, further improvement can be achieved by constellation shaping, using either non-uniformly spaced constellations or uniformly spaced constellations with non-uniform probability distributions. In contrast, we do not expect shaping to be beneficial at large L, where binary signaling per dimension (such as PM-4-QAM) should be optimal.

TABLE II
COMPARISON OF GAPS TO CAPACITY FOR DIFFERENT FEC SCHEMES, CHANNEL TYPES, AND RESIDUAL DISPERSION VALUES

FEC scheme	Decoding scheme	Channel	Distance	RDPS (%)	Gap (dB)
BCH–LDPC	SDD	AWGN			0.9
RS–LDPC	SDD	AWGN			2.0
		Optical	Long	100	2.9
				3.1	2.7
			Short	100	3.9
				3.1	4.0
RS–RS	HDD	Optical	Short	100	6.6
				3.1	6.4

Second, the gaps at large L are greater than for the DVB-S2 Bose/Ray-Chaudhuri/Hocquenghem (BCH)–LDPC codes on AWGN channels, where the lowest rate codes have gaps to capacity of about 0.9 dB [8]. We have replaced the outer BCH codes of [8] with RS codes in order to provide stronger error correction capability, further reducing the error floor. Compared to the DVB-S2 BCH codes, the RS codes provide slightly higher coding gains (about 0.1 dB), but their lower rates, combined with the line code rate, correspond to an increase in the gap of about 0.8 dB, computed using Eq. (5). Accordingly, the gap to capacity for our lowest rate RS–LDPC codes on AWGN channels is estimated to be about 0.9 dB – 0.1 dB + 0.8 dB = 1.6 dB. This estimate is close to the actual gap observed in Fig. 5, which is about 2.0 dB. The performance gaps observed in dispersion-compensated and -uncompensated nonlinear optical systems are about 0.7 dB and 0.9 dB higher than the 2.0-dB gap on AWGN channels. These increases in the performance gap can be attributed, at least in part, to residual channel memory (for both signal and noise) caused by the combined effects of CD and nonlinearity. We expect that these gaps can be reduced by using digital backward propagation, as was used in [27].

Third, using our SDD scheme, the performance gaps at small L are about 2.5 dB smaller than for the HDD scheme in [3], close to the expected advantage of SDD over HDD [28]. These gaps are measured at the longest distances where the highest information bit rate R_b (200 Gbit/s) is achievable, as shown in Fig. 8. It is less relevant to compare the schemes at large L, because the HDD scheme in [3] used repetition coding, which is known to be sub-optimal.

The proposed rate-adaptive scheme enables transmission over a very wide range of SNRs and over long distances, where high values of accumulated dispersion can affect the laser linewidth requirements [29]. Hence, we have evaluated the laser linewidth requirements, applying the same analysis as in [3]. We find worst-case linewidth requirements of about 2.6 MHz and 800 kHz for dispersion-compensated and -uncompensated systems, respectively. These requirements are similar to those in [3], and can be met using commercially available lasers [30].

In our simulations, we have assumed perfect carrier phase synchronization, and did not implement any specific carrier recovery algorithm. It is of crucial importance to mitigate cycle slips in carrier recovery. Systems using HDD FEC typically employ differential encoding of FEC-encoded bits at the transmitter and perform differential decoding of hard-decision bits prior to FEC decoding at the receiver [31]. The proposed scheme, as it uses SDD FEC, cannot rely upon differential encoding/decoding, but it can use the carrier recovery algorithms studied in [32], which prevent cycle slips.

VI. Conclusions

We have studied a rate-adaptive transmission scheme using variable-rate FEC codes, variable signal constellations, and a fixed symbol rate. The FEC scheme employs a family of concatenated RS codes (with HDD) and LDPC codes (with iterative SDD). We have combined the FEC scheme with single-carrier PM-M-QAM with varying M and digital coherent detection, evaluating performance in a model long-haul system with and without inline dispersion compensation. With zero SNR margin, information bit rates of 200/100/50/20 Gbit/s are achieved over distances of 960/2800/4400/9680 km and 1920/4960/8160/19,360 km for dispersion-compensated and -uncompensated systems, respectively. Compared to an ideal coding scheme achieving information-theoretic limits on an AWGN channel, the proposed scheme exhibits a performance gap ranging from about 4.0 dB at 960 km to 2.7 dB at 9680 km for dispersion-compensated systems, and from about 3.9 dB at 1920 km to 2.9 dB at 19,360 km for dispersion-uncompensated systems. The larger gap at short distances can be attributed to sub-optimality of the uniform QAM constellations, as compared to optimal Gaussian-distributed constellations. Some of the gap at large distances may be explained by residual channel memory (for both signal and noise), caused by the combined effect of CD and nonlinearity. Compared to a reference system using an HDD FEC scheme, we observed approximately 50% increases in transmission distance, and approximately 2.5-dB reductions in the performance gap from an ideal coding scheme.

In this work, we have considered only a single-channel system with intrachannel nonlinearities, in order to keep the simulation run time reasonable. If we included effects of interchannel nonlinearities, we would expect a reduction in the maximum distance at which a given bit rate can be achieved, but the results will not change qualitatively, because interchannel and intrachannel nonlinearities scale similarly with transmission distance. In previous work [3], we found that, in a three-channel system, interchannel effects cause about a 10% reduction in achievable transmission distance. Here, we have simulated SDD in floating-point arithmetic. We would expect a slight performance loss (less than 0.2 dB on an AWGN channel) when implementing a fixed-point decoder [33].

Acknowledgments

We thank Ori Gerstel of Cisco Systems for suggesting this research topic. This work was supported, in part, by a Google Research Award.

References

[1] O. Gerstel, M. Jinno, A. Lord, and S. J. Ben Yoo, "Elastic optical networking: A new dawn for the optical layer?" *IEEE Commun. Mag.*, vol. 50, pp. 12–20, Feb. 2012.

[2] G. Gho, L. Klak, and J. M. Kahn, "Rate-adaptive coding for optical fiber transmission systems," *J. Lightwave Technol.*, vol. 29, no. 2, pp. 222–233, Jan. 2011.

[3] G. Gho and J. M. Kahn, "Rate-adaptive modulation and coding for optical fiber transmission systems," *J. Lightwave Technol.*, vol. 30, no. 12, pp. 1818–1828, June 2012.

[4] T. Mizuochi, "Next generation FEC for optical communication," in *Opt. Fiber Commun. Conf.*, San Diego, CA, Feb. 2008.

[5] T. Mizuochi, Y. Miyata, T. Kobayashi, K. Ouchi, K. Kuno, K. Kubo, K. Shimizu, H. Tagami, H. Yoshida, H. Fujita, M. Akita, and K. Motoshima, "Forward error correction based on block turbo code with 3-bit soft decision for 10 Gb/s optical communication systems," *IEEE J. Sel. Top. Quantum Electron.*, vol. 10, no. 2, pp. 376–386, Mar./Apr. 2004.

[6] B. Vasic and I. Djordjevic, "Low-density parity-check codes for long-haul optical communication systems," *IEEE Photon. Technol. Lett.*, vol. 14, pp. 1208–1210, Aug. 2002.

[7] M. Arabaci, I. B. Djordjevic, L. Xu, and T. Wang, "Nonbinary LDPC-coded modulation for rate-adaptive optical fiber communication without bandwidth expansion," *IEEE Photon. Technol. Lett.*, vol. 24, pp. 1402–1404, Aug. 2012.

[8] *ETSI EN 302 307 V1.2.1*, Digital Video Broadcasting (DVB); Second Generation Framing Structure, Channel Coding and Modulation Systems for Broadcasting, Interactive Services, News Gathering and Other Broadband Satellite Applications (DVB-S2), Aug. 2009.

[9] Y. Miyata, W. Matsumoto, H. Yoshida, and T. Mizuochi, "Efficient FEC for optical communications using concatenated codes to combat error-floor," in *Optical Fiber Communication Conf./Nat. Fiber Optic Engineers Conf. (OFC/NFOEC)*, San Diego, CA, Feb. 24–28, 2008.

[10] P. K. Vitthaladevuni, M.-S. Alouini, and J. C. Kieffer, "Exact BER computation for cross QAM constellations," *IEEE Trans. Wireless Commun.*, vol. 4, no. 6, pp. 3039–3050, Nov. 2005.

[11] R. G. Gallager, *Low-Density Parity-Check Codes*. MIT Press, Cambridge, MA, 1963.

[12] T. Richardson, "Error floors of LDPC codes," in *Proc. of the Allerton Conf. on Communications, Control, and Computing*, Monticello, IL, Oct. 1–3, 2003.

[13] S. B. Wicker, *Error Control Systems for Digital Communication and Storage*. Prentice Hall, Englewood Cliffs, NJ, 1995.

[14] M. Yang and W. E. Ryan, "Lowering the error-rate floors of moderate-length high-rate irregular LDPC codes," in *IEEE Int. Symp. on Information Theory*, Yokohama, Japan, June 2003.

[15] D. J. C. MacKay, "Good error correcting codes based on very sparse matrices," *IEEE Trans. Inform. Theory*, vol. 45, no. 2, pp. 399–431, Mar. 1999.

[16] J. Ha, J. Kim, and S. W. McLaughlin, "Rate-compatible puncturing of low-density parity-check codes," *IEEE Trans. Inf. Theory*, vol. IT-50, pp. 2824–2836, Nov. 2004.

[17] T. Tian, C. Jones, and J. D. Villasenor, "Rate-compatible low-density parity-check codes," in *Proc. of IEEE Int. Symp. on Information Theory*, Chicago, IL, June 2004.

[18] J. Li and K. R. Narayanan, "Rate-compatible low-density parity-check codes for capacity-approaching ARQ schemes in packet data communications," in *Proc. of Int. Conf. Communications, Internet, and Information Technology*, St. Thomas, Virgin Islands, USA, Nov. 2002, pp. 201–206.

[19] G. Yue, X. Wang, and M. Madihian, "Design of rate-compatible irregular repeat accumulate codes," *IEEE Trans. Commun.*, vol. 55, no. 6, pp. 1153–1163, June 2007.

[20] *ITU-T G.975*, Forward Error Correction for Submarine Systems, Nov. 1996.

[21] G. D. Forney Jr., "Trellis shaping," *IEEE Trans. Inf. Theory*, vol. 38, pp. 281–300, Mar. 1992.

[22] A. R. Calderbank and L. H. Ozarow, "Nonequiprobable signaling on the Gaussian channel," *IEEE Trans. Inf. Theory*, vol. 36, pp. 726–740, July 1990.

[23] G. Caire, G. Taricco, and E. Biglieri, "Bit-interleaved coded modulation," *IEEE Trans. Inf. Theory*, vol. 44, no. 3, pp. 927–946, May 1998.

[24] E. Ip and J. M. Kahn, "Digital equalization of chromatic dispersion and polarization mode dispersion," *J. Lightwave Technol.*, vol. 25, no. 8, pp. 2033–2043, Aug. 2007.

[25] O. V. Sinkin, R. Holzlöhner, J. Zweck, and C. R. Menyuk, "Optimization of the split-step Fourier method in modeling optical-fiber communications systems," *J. Lightwave Technol.*, vol. 21, no. 1, pp. 61–68, Jan. 2003.

[26] M. Arabaci, I. B. Djordjevic, T. Schmidt, R. Saunders, and R. M. Marcoccia, "Rate-adaptive nonbinary-LDPC-coded modulation with backpropagation for long-haul optical transport networks," in *Int. Conf. on Transparent Optical Networks*, Munich, Germany, June 27–July 1, 2010, We.D1.5.

[27] R.-J. Essiambre, G. Kramer, P. J. Winzer, G. J. Foschini, and B. Goebel, "Capacity limits of optical fiber networks," *J. Lightwave Technol.*, vol. 28, no. 4, pp. 662–701, Feb. 2010.

[28] S. Benedetto and G. Bosco, "Channel coding for optical communications," in *Optical Communication: Theory and Techniques*. E. Forestieri, Ed., Springer, New York, 2005, pp. 63–78, ch. 8.

[29] W. Shieh and K.-P. Ho, "Equalization-enhanced phase noise for coherent-detection systems using electronic digital signal processing," *Opt. Express*, vol. 16, no. 20, pp. 15718–15727, Sept. 2008.

[30] J. P. Wilde, G. W. Yoffe, and J. M. Kahn, "Frequency noise characterization of a widely tunable narrow-linewidth DFB laser array source," in *Optical Fiber Communications Conf.*, San Diego, CA, Mar. 22–26, 2009.

[31] E. Ip and J. M. Kahn, "Feed-forward carrier recovery for coherent optical communications," *J. Lightwave Technol.*, vol. 25, no. 9, pp. 2675–2692, Sept. 2007.

[32] E. Ip and J. Kahn, "Addendum to feedforward carrier recovery for coherent optical communications," *J. Lightwave Technol.*, vol. 27, no. 13, pp. 2552–2553, July 2009.

[33] R. Zarubica, R. Hinton, S. G. Wilson, and E. K. Hall, "Efficient quantization schemes for LDPC decoders," in *Proc. of the IEEE Military Communications Conf.*, San Diego, CA, Nov. 2008.

Gwang-Hyun Gho received his B.S. degree in Electronics Engineering from Korea University, Seoul, South Korea, in 1995, and his M.S. and Ph.D. degrees in Electrical Engineering from Stanford University, Stanford, CA, USA, in 1999 and 2011, respectively. From 1999 to 2005, he was at Qualcomm Inc., Campbell, CA, where he developed WCDMA and HSDPA modems as a systems engineer. From 2005 to 2009, he was a DSP engineer at Amicus Wireless Technology Inc., Sunnyvale, CA, developing mobile WiMAX modems. Since 2011 he has been developing LTE modems at Qualcomm Inc., Santa Clara, CA, as a firmware engineer. His research interests include optical and wireless communications, error control coding, and digital signal processing.

Joseph M. Kahn (M'90–SM'98–F'00) received his A.B., M.A., and Ph.D. degrees in Physics from U.C. Berkeley in 1981, 1983, and 1986, respectively. From 1987 to 1990, he was at AT&T Bell Laboratories, Crawford Hill Laboratory, in Holmdel, NJ, USA. He demonstrated multi-Gbit/s coherent optical fiber transmission systems, setting world records for receiver sensitivity. From 1990 to 2003, he was on the faculty of the Department of Electrical Engineering and Computer Sciences at U.C. Berkeley, performing research on optical and wireless communications. Since 2003, he has been a Professor of Electrical Engineering at Stanford University, where he heads the Optical Communications Group. His current research interests include rate-adaptive and spectrally efficient modulation and coding methods, coherent detection and associated digital signal processing algorithms, digital compensation of fiber nonlinearity, high-speed transmission in multimode fiber, and free-space systems. Professor Kahn received the National Science Foundation Presidential Young Investigator Award in 1991. He is a Fellow of the IEEE. From 1993 to 2000, he served as a Technical Editor of *IEEE Personal Communications Magazine*. Since 2009, he has been an Associate Editor of the IEEE/OSA *Journal of Optical Communications and Networking*. In 2000, he helped found StrataLight Communications, where he served as Chief Scientist from 2000 to 2003. StrataLight was acquired by Opnext, Inc. in 2009.